Chapter 3

Development of Real-Time Sensing Network and Simulation on Air Pollution and Transport

Yasuko Yamada Maruo and Akira Sugiyama

Additional information is available at the end of the chapter

http://dx.doi.org/10.5772/39269

1. Introduction

This chapter describes an air quality-monitoring project carried out in Metro Manila in the Philippines in 2006. We developed a real-time environmental and atmospheric sensing system and used it to measure air pollution and weather parameters remotely in order to simulate the gathered data with a 3D fluid simulator and another simulation model. Traffic count surveys were also conducted to acquire road traffic data to allow us simulate traffic density and traffic flow.

In urban areas of the Philippines, industrialization and the rapid growth of motorization has caused serious environmental problems to local residents (Lodge, 1992; Isidrovaleroso et al., 1992). In this study we established a system and methodology for monitoring air pollution in real time and to evaluate related environmental aspects by using the latest sensing network technology. For this project, we used a small nitrogen dioxide (NO_2) sensor and a suspended particulate matter (SPM) sensor, both of which we developed. These air pollutant sensors can perform real-time monitoring at several monitoring points along a road network. SPM has recently been recognized as an air pollutant that has a causal correlation with the human fatality rate (Sabin et al., 2005), and NO_2 is recognized as an air pollutant that causes respiratory illness (Smith et al., 2000). In conventional studies, air pollutant amounts are measured with passive samplers that require very longer measurement periods of up to a month, and no dynamic validation has been conducted in real time. The air pollutant concentration will fluctuate widely over short intervals and the weekly/monthly average concentration could be far lower than the actual daily peak. Macroscopic and microscopic transportation and environment models have been developed to predict the pollutant concentration from the aggregate transportation demand and traffic flow simulations, but there has been no dynamic validation of the pollutant concentrations. By measuring pollutant concentrations and weather parameters at ten- or sixty-minute

intervals, the daily variation can be measured and the correlation between pollutant concentration, weather parameters and traffic volume can be simulated.

The results obtained with the simulation system will be useful for the evaluation and implementation of urban transportation policies, pollution countermeasures, guidelines and human resource programs. The environmental impact of policies and social experiments can be directly with an SPM and NO_2 measurement network system, which will be very useful for policymakers and decision-makers in national and local government agencies.

2. Development of real-time sensing network

2.1. System outline

A real-time sensing network system was established with the following process:

- The observation data are periodically transferred over a cell-phone (GPRS) from the sensors installed along an arterial road in Metro-Manila to Server I (PH-SV) in which they are stored.
- The data stored in PH-SV are periodically transmitted to Server II (JP-SV) over the Internet, and stored.
- In JP-SV, raw SPM data are converted into mass density ($\mu g/m^3$), and NO_2 data are converted into concentration (ppb) using the above-mentioned arithmetic expression.

In JP-SV, the calculated data are stored in RDBMS (PostqreSQL) and the WEB application provides some functions (time-series graphs of SPM and NO_2, data search and data download, etc.). By employing these functions, these data can be accessed from anywhere and at any time via a PC that is connected to the Internet. The data measured and output by a weather sensor are understandable as they are, so they do not need to be processed with an arithmetic expression. The outline of our project is shown in Fig. 1.

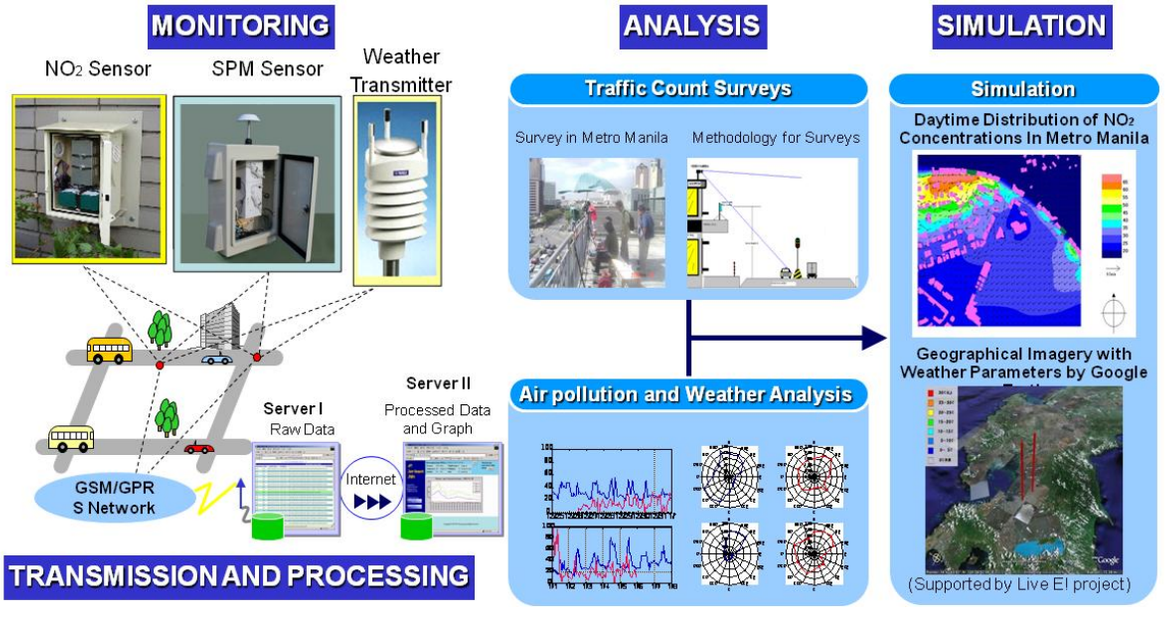

Figure 1. Outline of this research

2.2. System diagram

A chart showing the composition of the entire system is shown in Fig. 2. In this section, we describe each mechanism of the system separately. The system is divided into the following four parts:

1. Sensor to PH-SV: Transfer each sensor's measurement data (raw data) to PH-SV over the GSM/GPRS wireless with a controller programming method.
2. PH-SV to JP-SV: Transfer the raw data from PH-SV to JP-SV over the Internet with a UNIX secure protocol.
3. Calculation application: On JP-SV, calculate the raw data into concentrations by using each expression and store them in a database.
4. Web application: Provide certain functions (e.g. graph view, data selection and data download) for web application.

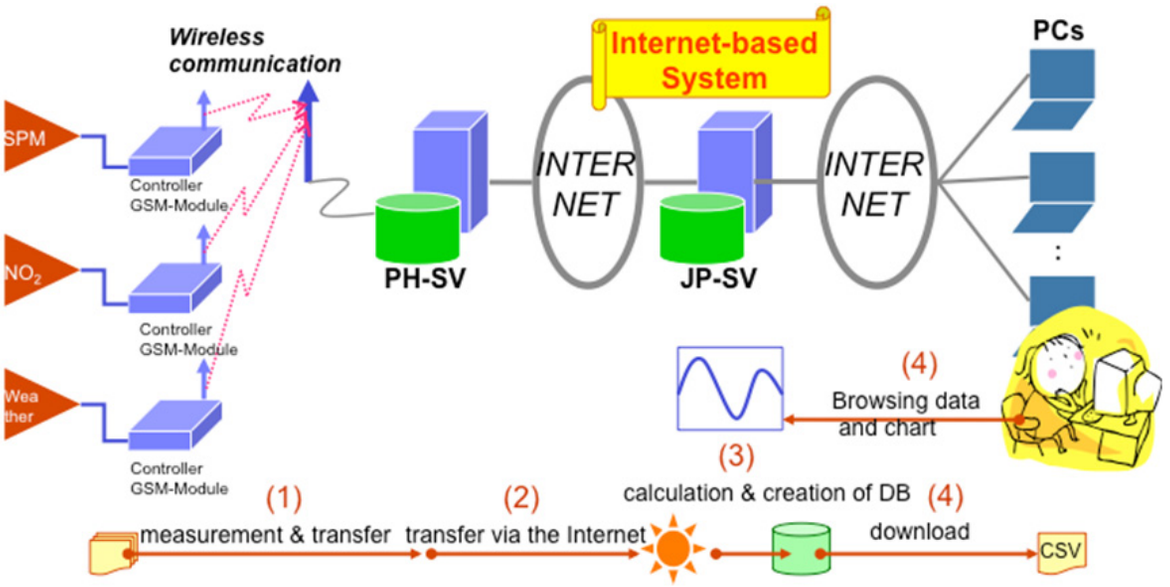

Figure 2. System diagram of this research

2.3. Principles and performance of environmental sensors

2.3.1. NO_2 sensor

The NO_2 sensor is an accumulation type sensor (Tanaka et al. 1999). The sensor element that detects NO_2 has a reagent contained in porous glass that reacts chemically only with a particular gas (diazo coupling reaction) as shown in Fig. 3 (a). This sensor consists of 1-mm thick porous glass sheets with an average pore diameter of 4.6 nm, a vacancy ratio of 28%, and a specific surface area of 195 m^2/g, cut into 8 x 8 mm chips. After exposure to ambient NO_2, the chips turn pink. A specific single absorption peak appears at 525nm and it is clear that the absorbance increases as the exposure time increases. This pink material is stable and there is no change in the absorbance after the preservation of the exposed samples in a dry nitrogen atmosphere. The NO_2 concentration was calculated from the absorbance difference at 525 nm and the exposure time.

2.3.2. NO_2 monitoring device

A device has been developed that can detect low levels of NO_2 gas (Maruo et al. 2003). The device consists of a sensor element, an absorbance meter with a single wavelength (525 nm) light source, a controller containing a data converter and a mobile modem to make it possible to transfer data from the device to a central PC through a wireless network. The device is outlined in Fig. 3 (b). It is very compact with dimensions of 200 mm W x 100 mm D x 85 mm H. Another feature of the device is that it has no pumping unit for replacing the air above the sensor. Instead, the body includes an electric heater (electric board) to provide a convection flow and several slits for ventilation. It is possible to calculate the ventilation speed using a simple structural model and factors related to the energy consumption of the electric board and the difference between the temperatures outside and inside the device. This gives a value of about 1l/min indicating that the inside air is replaced in <1.5 min.

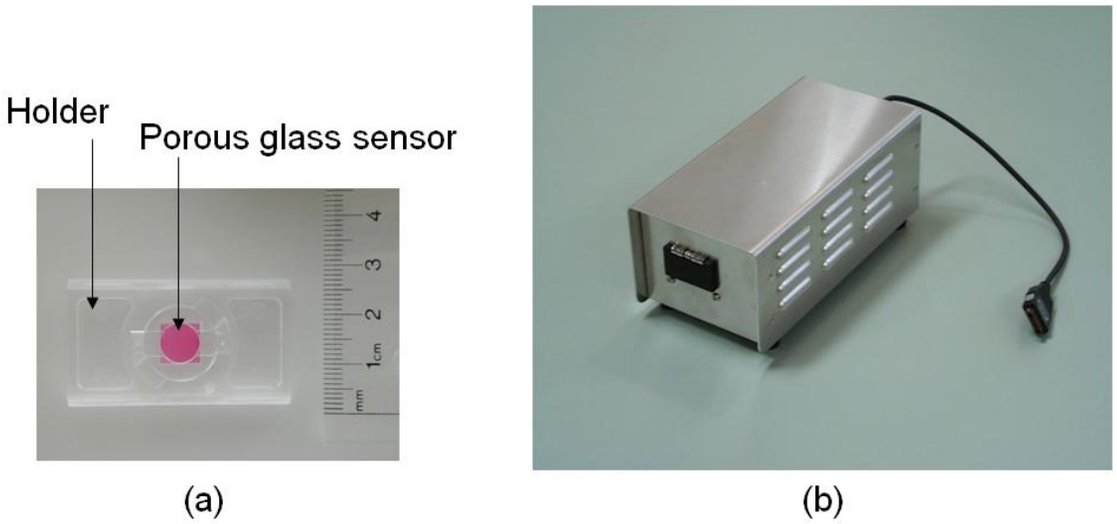

Figure 3. Photographs of developed NO_2 monitoring system. (a) NO_2 sensor element, (b) NO_2 monitoring device.

2.3.3. SPM sensing device

A suspended particulate matter (SPM) sensing device has been developed (Tanaka, et al., 2004) and used to measure the relative SPM concentration in ambient air with the right-angle light scattering method according to the particle diameter at the time the particles pass through it. SPM is thought to be a cause of respiratory ailments such as asthma, because it can easily reach the respiratory organs. In this study, we set up this compact SPM sensor with a GSM/GPRS network module along with an NO_2 sensor and a weather transmitter (WXT520, VAISALA) to develop a real-time sensing network.

As illustrated in the Fig. 4, this SPM sensor employs an optical particle counter based on the right-angle light scattering caused by suspended particles, and determines the number of particles and their diameter. By combining a dilutor with a particle counter, high SPM concentrations can be detected up to a maximum of 12,000 particles/cc. Since the amount of light that is scattered depends on the particle size, a pulse-height analyzer makes it possible

to count particles classified into five diameter ranges, namely 0.3-0.5, 0.5-1.0, 1.0-2.5, 2.5-7 and 7-10 μm, according to the scattered light pulse intensity.

The SPM sensor used here is less than one tenth the size of conventional SPM monitoring instruments.

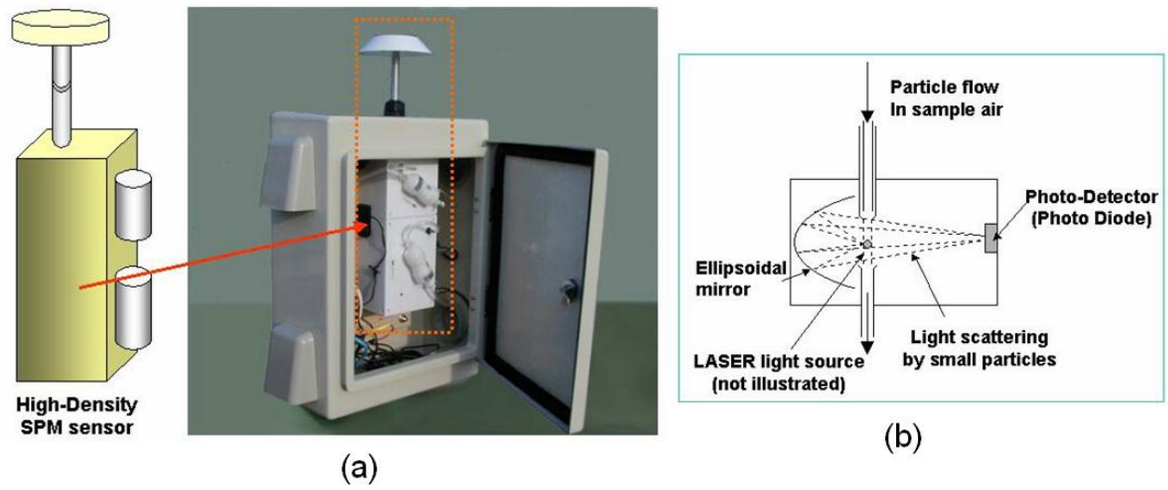

Figure 4. Photographs of developed SPM monitoring system. (a) SPM sensing device, (b) particle detection method.

3. Experiment in Metro Manila

3.1. Outline of experiment

In this study, we established three monitoring. Of these monitoring points, two were beside a busy thoroughfare within the Makati Commercial Business District (Makati CBD) to study the variation in air pollution effected by street canyons and traffic on the road. While the third monitoring point focused on the background conditions used for running the simulation study.

The equipment employed for the study consisted of two NO_2 monitoring devices, one SPM sensing device, and two weather stations. One NO_2 sensor, one SPM sensor and one weather station were prepared for roadside installation in the Makati CBD. The remaining NO_2 sensor and weather station were used to collect background data.

The weather stations should be more than 5 meters above the roof deck. This is because, in this study, the representative wind velocity of the monitoring point is measured by the weather station and the measurement should be 5 meters above the roof deck or side wall of a building to avoid the influence of the boundary layer from those objects.

The Intellectual Property Office (IPO) Building and the Board of Investments (BOI) Building, both on Senator Gil J.Puyat Avenue in the Makati CBD in Metro Manila were selected as the locations of the first two monitoring points for the study. And both have canopies over their front entrances that jut out towards the roadside and over which the SPM and NO_2 sensors were easily mounted.

Both buildings also have roof decks that have no street canyon effect. Therefore, portable weather stations can be installed on those roof decks to provide wind speed, wind direction, air temperature, air pressure, relative humidity, and precipitation data. The third monitoring point is located inside the National Mapping and Resource Information Authority (NAMRIA) compound inside the Fort Bonifacio military reservation less than 6 km south east of the first two monitoring points.

Figure 5. Real time monitoring devices

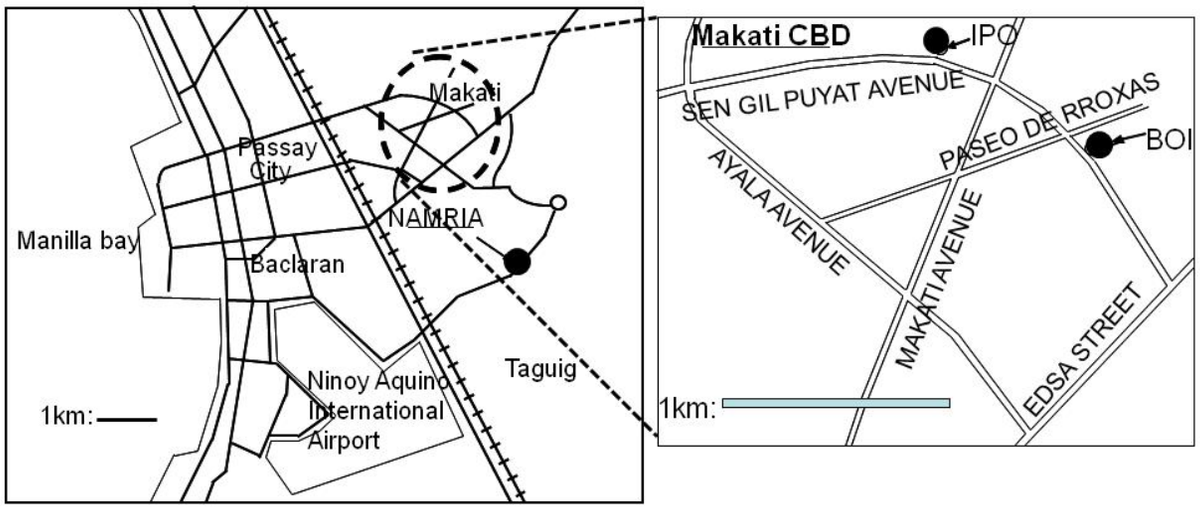

Figure 6. Air monitoring locations in the Manila and in Makati CBD.

3.2. Monitoring point; IPO

The IPO building is located on Senator Gil J.Puyat Avenue about 300 meters far from its corner with Makati Avenue. The road in front of the IPO has six lanes and is about 22 meters

wide, and the IPO is in a street canyon. The IPO building also has a canopy that induces a street canyon effect. NO_2 and SPM sensors were mounted on the canopy because it is 3 meters above the ground. The IPO building also has an accessible roof deck, but there is a wall on the roof deck. To avoid the boundary layer and turbulences caused by this wall, the weather station was mounted on the top of a pole that was fixed to handrails.

Figure 7. Photographs of roadside monitoring points; IPO. (a) The Senator Gil J.Puyat Avenue and IPO building, (b) NO_2 monitoring device and SPM sensing device, (c) weather station.

3.3. Monitoring point; BOI

The BOI building is also located along Senator Gil J.Puyat Avenue. The road in front of the BOI also has six lanes and is about 22 meters wide. The BOI building is not in a street canyon but in an open space. The NO_2 sensor and the SPM sensor were installed at the top of the canopy at a height of 3meters.The canopy and therefore the sensors are 3 meters away from the vehicular road. The BOI building also has a roof deck that we can access, but there is a structure on the roof deck. To avoid the boundary layer and turbulences induced by this structure, the weather station was set on the top of a pole that was fixed to the handrails of the structure.

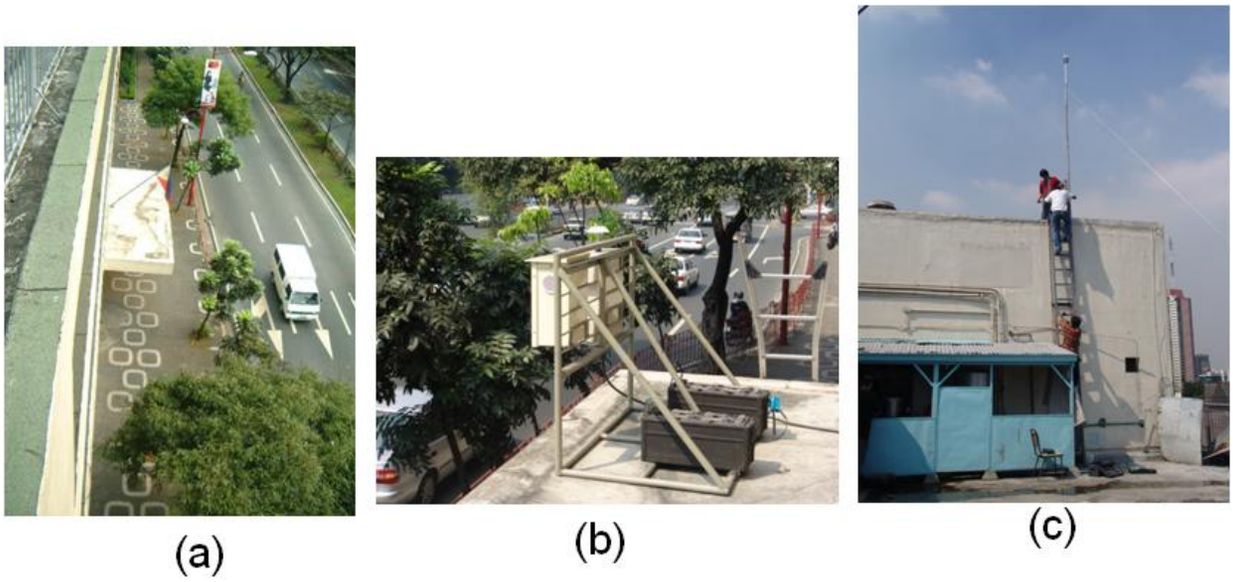

Figure 8. Photographs of roadside monitoring point; BOI. (a) The Senator Gil J.Puyat Avenue and BOI building, (b) NO_2 monitoring device and SPM sensing device, (c) weather station.

3.4. Monitoring point; NAMRIA

NAMRIA is located along McKinley Road. The road has four lanes and is 12 meters wide. To avoid the air pollution from McKinley Road, the NO_2 sensor was mounted on the roof of a security office more than 150 meters from the road. The roof is only 3 meters above the ground but there is adequate security so the NO_2 sensor was set on the roof of the security office. The weather station was installed on the top of a pole, which was raised on the roof deck of the NAMRIA building.

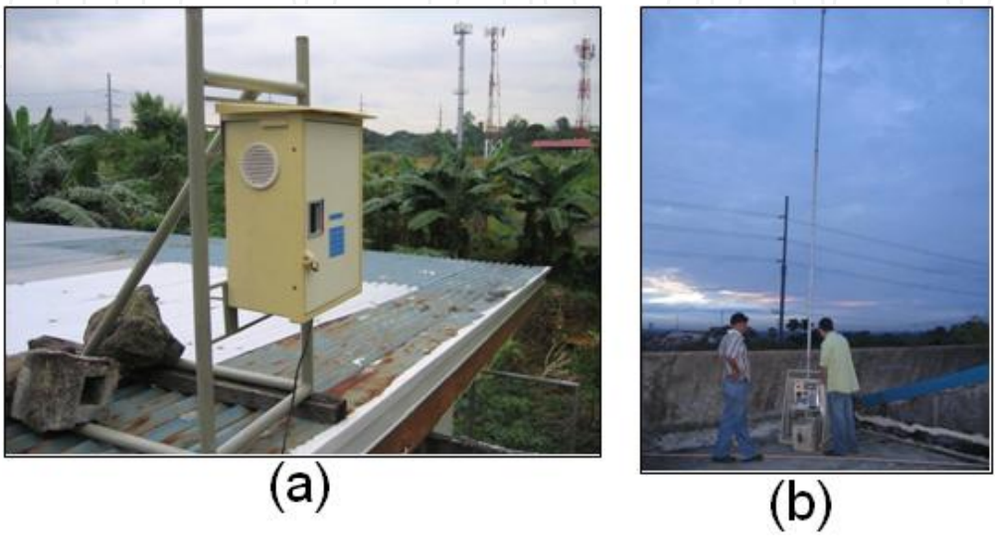

Figure 9. Photographs of background monitoring point; NAMRIA. (a) NO_2 monitoring device, (b) weather station.

3.5. Measurement schedule

In this study, measurements were gathered for over 2 weeks at each monitoring site, IPO and BOI. Two NO_2 sensors, one SPM sensor and two weather stations were mounted along the time schedule indicated in the table 1.

Month/Year	12/2005				1/2006					2/2006	
Day	5	12	19	26	2	9	16	23	30	6	13
SPM		IPO				BOI					
NO_2-1		IPO				BOI					
NO_2-2			NAMRIA								
Wet.-1		IPO				BOI					
Wet.-2			NAMRIA								

Table 1. Time schedule of measurement

4. Methodology for traffic surveys

4.1. Traffic counts

Traffic volume, defined as the number of vehicles passing a predetermined observation line during a certain time period, is a very important variable with regard to obtaining the relationship and the degree of traffic involvement with in-situ concentrations of particulate and gaseous pollutants in a roadside environment.

In this project, traffic volume was determined at a midblock section and an intersection. Monitoring at the first location involved establishing an observation line across the road of interest and locating it directly in front of the sensors. We then counted the number of vehicles that crossed the line during a pre-set time period of 3-4 hours for peak observations (4 hours in the morning and another 3 hours in the afternoon) 2 hours at night and 2 hours for off-peak observations. A video camera was mounted on top of the IPO and BOI buildings to record the traffic and counts were measured later (not in real time). The typical set-up is shown in Fig. 10.

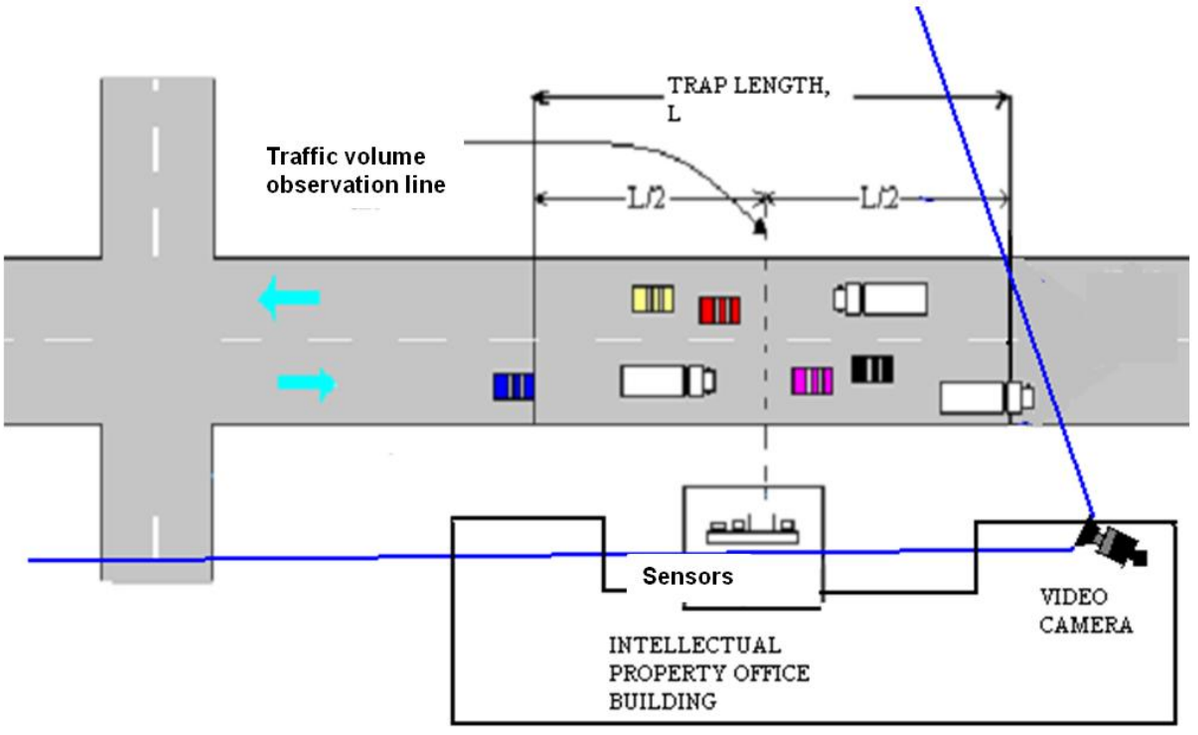

Figure 10. Plan view of traffic surveys set-up.

The survey was scheduled to be undertaken on at least one weekday and one weekend (Sunday) during the following time periods:

- 6:00 AM – 10 AM (AM peak)
- 11:00 AM – 2 PM (daytime off-peak)
- 4:00 PM – 7 PM (PM peak)
- 2:00 AM – 4:00 AM (nighttime off-peak)

Vehicle classifications for the traffic counts include the following:

(1) passenger car, (2) light truck, (3) private jeepney, (4) van, (5) medium truck, (6) minibus, (7) taxi, (8) heavy truck, (9) bus, (10) FX taxi, (11) public utility jeepney, and (12) motorcycle/tricycle

4.2. Vehicle speed surveys

Vehicle speed, generally referred to as the distance in kilometers that a point on a vehicle travels per hour of elapsed time, is as important as traffic volume because different speeds will yield different emission levels, resulting in varying amounts of pollutant deposition. It is for this purpose that the speeds of vehicles traversing the road were obtained for later association with traffic volume and pollutant emissions for modeling studies.

5. Results of experiment

5.1. Results of traffic count surveys

Traffic surveys were conducted on four days:

- January 5, 2006 [along Sen. Gil Puyat Avenue at IPO Building]
- January 8. 2006 [along Sen. Gil Puyat Avenue at IPO Building]
- January 18, 2006 [along Sen. Gil Puyat Avenue at BOI Building]
- January 22, 2006 [along Sen. Gil Puyat Avenue at BOI Building]

The raw data for each day were encoded and processed for the morning and afternoon peak periods as well as the noontime off-peak period. Sample outputs from the surveys are shown in Fig. 11.

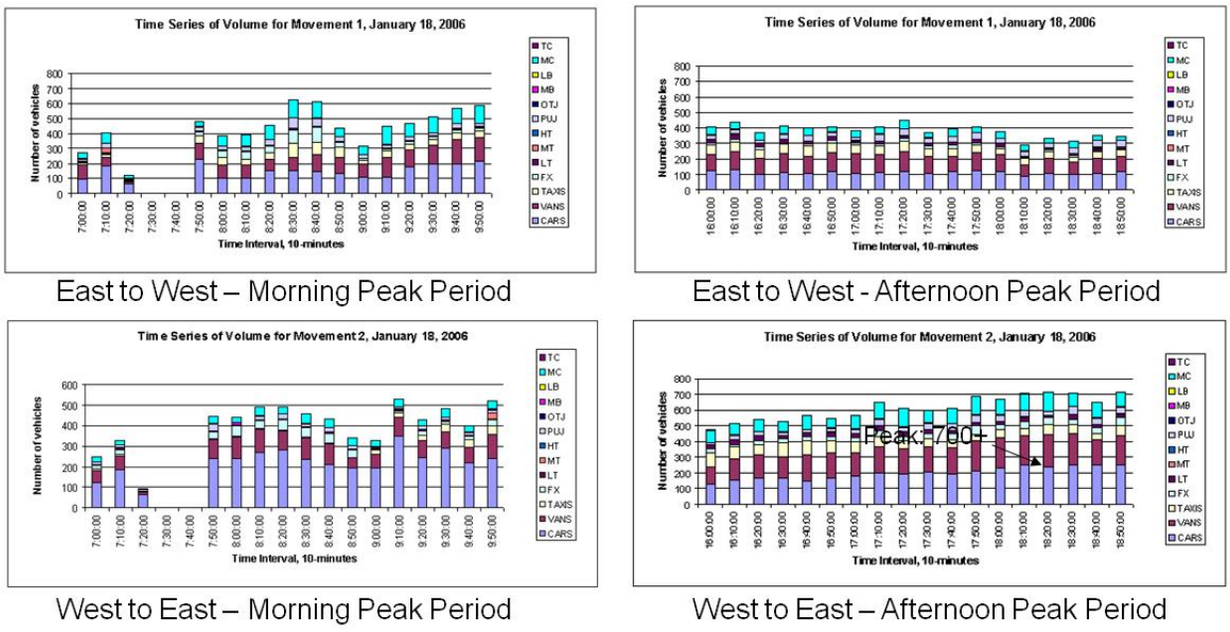

Figure 11. Variations in traffic volume along the Sen. Gil Puyat Avenue on 18 Jan (Wed), 2006.

Speed samples were also derived from the field surveys. Example measurements are shown in Table 2.

Time Period			Speed	
			meter/sec	km/hr
6:10:00	-	6:15:00	7.6	27.5
6:15:00	-	6:20:00	8.8	31.7
6:20:00	-	6:25:00	9.6	34.6
6:25:00	-	6:30:00	9.1	32.6
6:30:00	-	6:35:00	11.8	42.6
6:35:00	-	6:40:00	10.8	39.0
6:40:00	-	6:45:00	9.3	33.3
6:45:00	-	6:50:00	9.1	32.7
6:50:00	-	6:55:00	9.6	34.7
6:55:00	-	7:00:00	11.1	39.8
7:00:00	-	7:05:00	11.0	39.7
7:05:00	-	7:10:00	11.6	41.6
7:10:00	-	7:15:00	9.5	34.3
7:15:00	-	7:20:00	8.3	29.7
7:20:00	-	7:25:00	10.4	37.6
7:25:00	-	7:30:00	10.0	35.8
7:30:00	-	7:35:00	9.6	34.6
7:35:00	-	7:40:00	11.0	39.4
7:40:00	-	7:45:00	10.2	36.6
7:45:00	-	7:50:00	9.7	34.9
7:50:00	-	7:55:00	8.1	29.0
7:55:00	-	8:00:00	8.9	32.1

Table 2. Sample speed measurements (Jan. 22, 2006/AM Peak/Direction towards Ayala Avenue).

5.2. NO_2 measurement results

Figure 12 shows examples of time-series plots of NO_2 concentrations obtained at two different points (IPO and NAMRIA). The experiment at IPO was performed between Dec. 16, 2005 and Jan. 9, 2006, and that at NAMRIA from Dec. 22, 2005 to Jan. 23, 2006. We used two NO_2 sensors; one was used for the measurement at NAMRIA and the other for the measurements at IPO and subsequently at BOI.

Data were acquired by a sensor and transferred to a server at one-hour intervals. Although some data were lost when the data collection failed, we were nevertheless able to measure the accumulated NO_2 concentration. This is because we used an accumulation type sensor as described above. The one-hour NO_2 concentration value for a period where data collection failed was calculated as a mean value. For example, we successfully collected data at 15:00 after failing for four hours (from 11:00 to 14:00 on Dec. 16, 2005). The accumulative NO_2

amount for five hours (from 11:00 to 15:00) was calculated at 242 ppb, giving a one-hour mean value of 48 ppb. In Fig. 12, the parts showing the mean values are indicated by A.

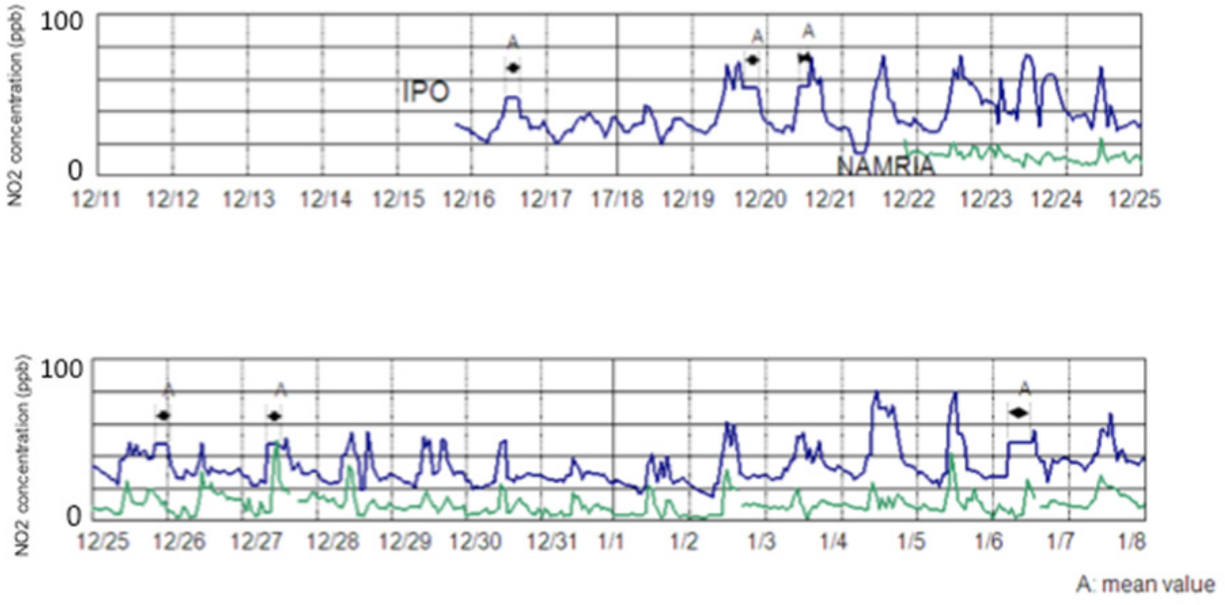

Figure 12. Time series plots of NO_2 concentrations at two different points (IPO and NAMRIA).

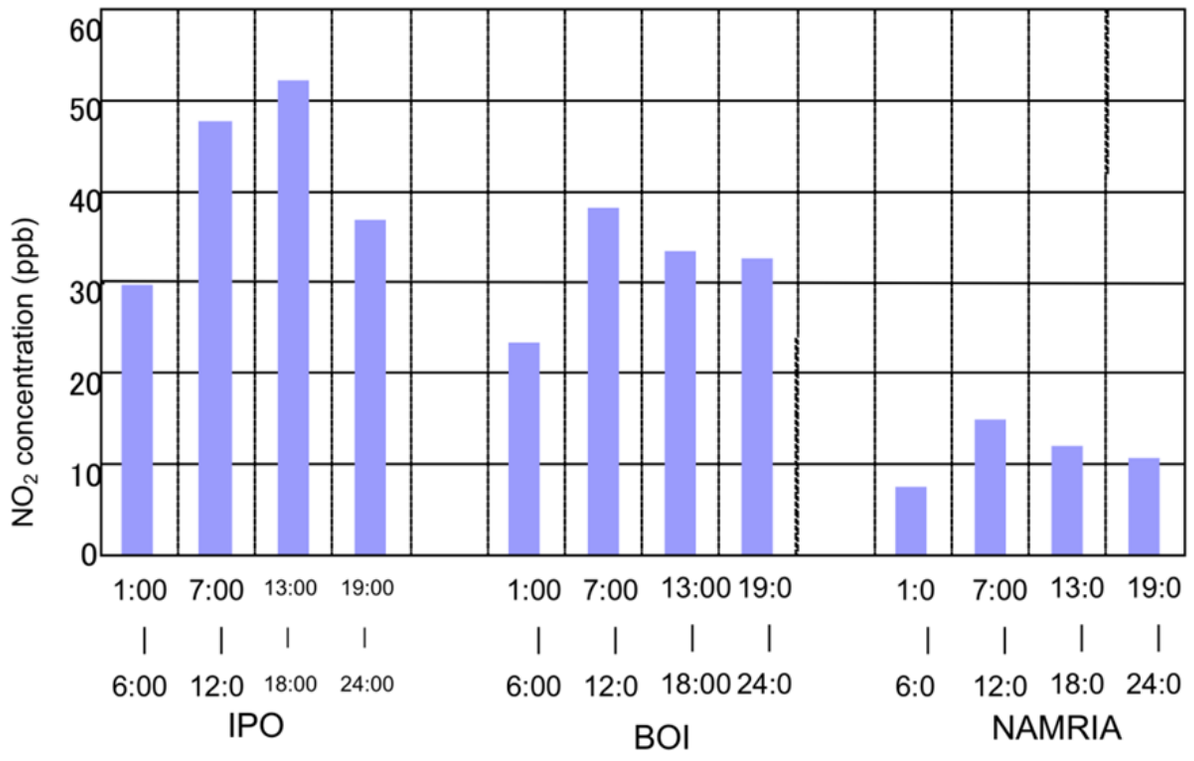

Figure 13. Calculated six-hour average NO_2 concentrations for weekdays at three points.

Figure 13 shows the six-hour average NO_2 concentration for weekdays at the three points. For both BOI and NAMRIA, the peak concentration hour appears during the second period (from 7:00 to 12:00), which corresponds to peak traffic hours. On the other hand, for IPO, the peak concentration hour appears during the third period (from 13:00 to 18:00), which does not correspond to peak traffic hours. The peak concentration hours for IPO appeared after those of both BOI and NAMRIA. We assume this to be because IPO is in a canyon. It has been reported that NO_2 becomes concentrated in canyon areas after peak traffic hours (Maruo et al. 2003).

5.3. SPM measurement results

Figure 14 shows time-series plots of SPM concentrations at a monitoring point (IPO). The experiment at IPO ran from Dec. 16, 2005 to Jan. 5, 2006. Since we had one SPM sensor set, we used it first for the measurement at IPO and then moved it to BOI. Data were acquired by the sensor and transferred to a server at ten-minute intervals.

The one-hour average SPM mass concentration for weekdays was about 25 % higher than the weekend concentration. The mass concentration was considerably smaller than the already reported value (Santos et al. 2006, Oanh et al., 2006). Figure 15 shows the six-hour average SPM mass concentration for weekdays at IPO. The peak concentration hours appear during the second period (from 7:00 to 12:00), which corresponds to peak traffic hours.

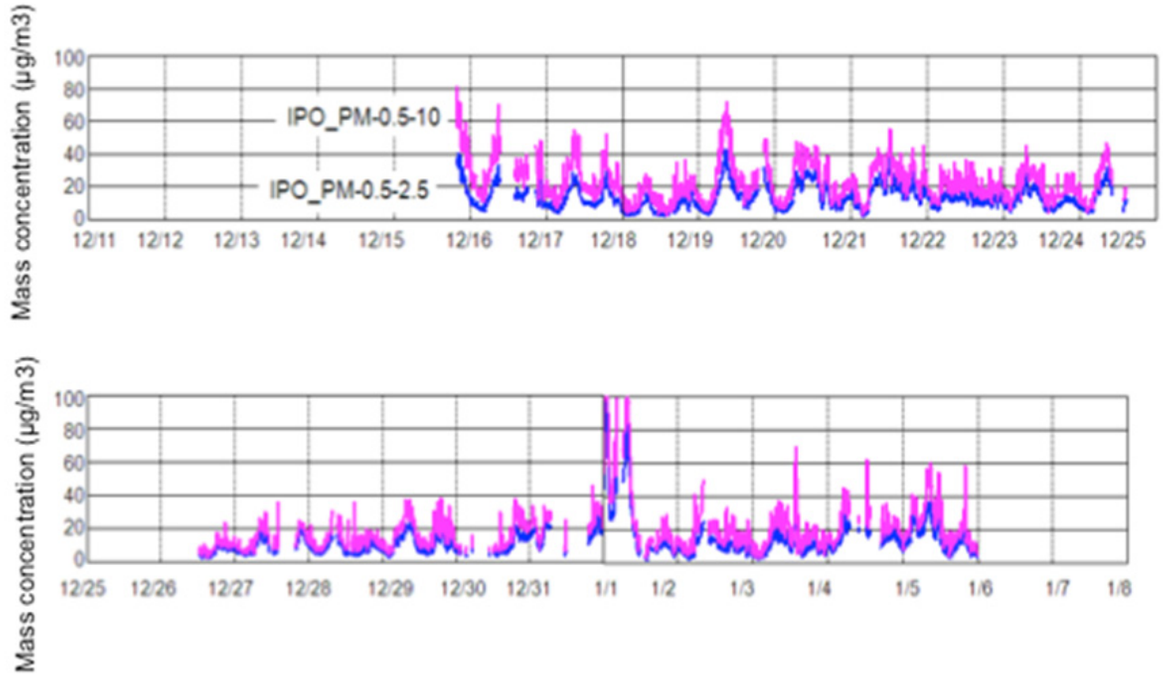

Figure 14. Time series plots of SPM concentrations at IPO. The high concentration on Jan. 1 was due to firecrackers being let off on the New Year's holiday.

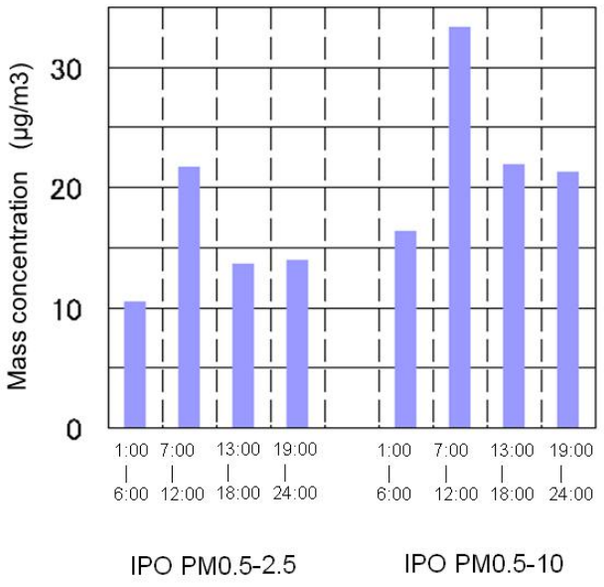

Figure 15. Calculated six-hour average SPM concentrations for weekdays at IPO.

6. Simulation and consideration

6.1. Objective of simulation

An analysis of the data we obtained from the sensors located on the IPO and the BOI buildings provided a lot of information about the SPM and NO_2 concentrations as described in section 5. Although these sensors gave us detailed information, it was only about the areas around their locations. It is difficult to infer what is happening in the target area around the Makati CBD solely from the sensor data.

A 3-D fluid simulator can show us what is happening in a target area better than sensors. We simulated pollutant concentrations using the data obtained from the sensors to understand which areas have high concentrations of pollutants in the Makati CBD and how wide these areas are. The results will be useful for evaluating and implementing urban transportation policies, pollution countermeasures, guidelines, and human resource programs. These results will also be very useful for policymakers and decision makers in national and local government agencies.

An analysis of the data obtained from the NO_2 sensor located on the IPO building showed that the NO_2 concentrations exceeded the Japanese environmental quality standard levels of 40 and 60 ppb (EQS, 2012). For public health reasons, it is preferable that NO_2 concentrations not exceed that standard. The distribution of the NO_2 concentration was calculated around the Makati CBD in this study, and regions where the NO_2 concentration exceeded 40 or 60 ppb were identified.

6.2. Model description

The 3-D localized atmospheric environment simulator is an integrated system that can consistently perform all the required processes ranging from collecting data, such as a map

model and initial conditions, to confirming the calculation results. The simulator is based on an air flow simulator developed by Kozo Keikaku Engineering, Inc. (KKE, 2012). A hydrodynamic method is used to calculate the advection and diffusion of pollutants in the atmosphere in three dimensions. This allows us to take account of the shapes and heights of buildings, which was not possible with conventional two-dimensional calculations. A 3-D computational domain can be easily made from a digital map that includes the shape and height of buildings and road networks. As a result, the simulator allows the calculation of the distributions of temperature, humidity, car exhaust emissions, heat radiated by buildings, etc. in an urban environment where wind flows are very complex. Numerical analysis by the finite volume method is used to solve the continuity equation that is derived from the assumption that the flow is a three-dimensional incompressible viscous flow, and from the Navier-Stokes, energy, and advective-diffusion equations.

The main characteristic of this 3-D fluid simulator (Tanaka et al., 2004) is that it calculates the photochemical reactions of pollutants and air flow simultaneously. Motor vehicle exhaust gas contains many air pollutants including NO and NO_2. NO reacts quickly with ozone to form NO_2. However, sunlight breaks down NO_2 via a photochemical reaction, so the simultaneous calculation of photochemical reactions and air flow makes it possible to simulate the NO_2 concentrations more precisely. We simulated the NO_2 concentration around the Makati CBD, and analyzed the simulation results to identify areas of high concentration.

6.3. Conditions and input parameters

Various parameters including wind conditions and the amount of air pollutants from motor vehicles should be established to simulate air pollutant concentrations by numerical analysis. The settings of these parameters are described in this section.

The NO_2 concentrations in the air near the IPO and BOI buildings fluctuated widely throughout the day as discussed in section 5. Although these fluctuations were more prominent because the sensors were located near the main road, the pollutant concentrations over the whole area fluctuated like those near the roadside. Since the purpose of the simulation was to identify the areas where the NO_2 concentration was high, and these areas varied based on the time of day, we selected three characteristic time periods when calculating the distribution of the NO_2 concentration:

1. low concentration: 2:00 – 3:00 AM,
2. high concentration: 11:00 AM – 12:00 PM,
3. many people are outdoors: 5:00 – 6:00 PM.

We calculated the most frequent wind direction and the average wind velocity and background concentration for each time period and we used all the data obtained in this experiment to calculate these average values and thus simulate the distribution of the NO_2 concentration under typical conditions in the Makati CBD in winter. Data gathered on weekends were excluded from the calculation of the average background concentrations because of the difference between weekends and weekdays. We simulated weekday conditions because the pollutant concentrations on weekdays were higher than those at weekends.

6.3.1. Computational domain

3-D and 2-D representations of the computational domain are shown in Fig. 16(a) and (b), respectively. This computational domain was made from a digital map that includes road networks, road widths, building shapes, and building heights. The size of the target area was 2.2 square kilometers, and the center was around the intersection of Makati and Sen. Gil Puyat Avenues. Sen. Gil Puyat Avenue is shown as a blue line and the IPO and BOI buildings are shown as green blocks.

An orthogonal grid system was applied. Its specifications are as follows.

1. Number of grids: 110 (x) X 110 (y) X 53 (z).
2. Width of grids: regular horizontal intervals at 20 m,regular vertical intervals at 1 m (up to 10 m high), irregular vertical intervals between 1 and 50 m (higher than 10 m).

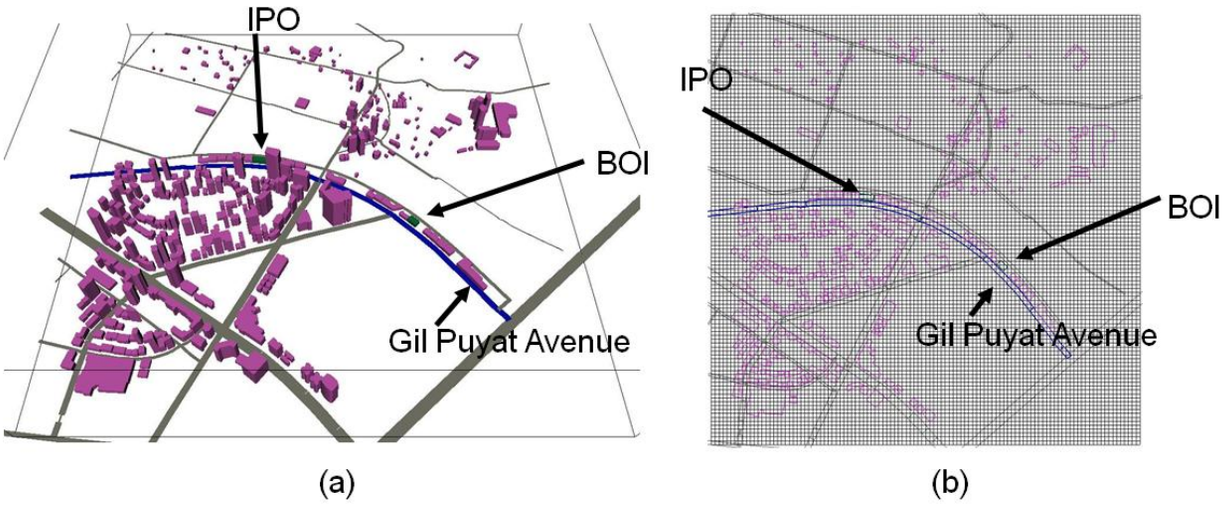

Figure 16. Calculation description of the Makati CBD, (a)3-D representation, (b)2-D representation and grid description

6.3.2. Sources

Motor vehicles that drive down Sen. Gil Puyat Avenue were considered to be sources of air pollution. Although the simulated NO_2 concentration distribution, which assumes that air pollutants are emitted from only one road, may differ from the actual distribution in the Makati CBD, we can identify the effect of air pollutants emitted from vehicles on the road. The volumes of emitted air pollutants were estimated from traffic volumes and vehicle speeds measured in this experiment. We used the emission factor proposed by the Asian Development Bank in 1992 (ADB, 1992). Although the 1992 emission factor is different from the current one, we assumed that the ADB emission factor is the most reliable one available in the Philippines. The vehicle classifications used with the ADB emission factor are different from those for the traffic counts in our experiment. The correspondence between the ADB vehicle classification and ours is shown in Table 3.

Classification in ADB	Classification in our experiment
Gas Car	Passenger car ,Van ,Taxi
Gas Jeep	Private Jeepney
Diesel Car	FX Taxi
Diesel Jeepny	Light Truck, Medium Truck, Public Utility Jeepney, Minibus
Diesel Bus	Heavy Truck ,Bus
Gas Tricycle	Motor Cycle, Tricycle

Table 3. Correspondence between ADB vehicle classification and our experimental classification

We calculated the NOx emission volume using the ADB emission factor. The NOx emission volume is the sum of the NO and NO_2 emission volumes. The NO and NO_2 emission volumes are needed to simulate the photochemical reaction process. Emission volumes of pollutants other than NOx, such as NMHC, are also needed. These emission volumes were estimated using the ratio of these emissions compared with the NOx emissions reported by Tange (Tange, H. et al. 1987). We used the traffic volume measured on January 5, 2006. Table 4 lists the traffic and the NOx emission volumes.

Time of day	Traffic Volume(10^{-4}vehicle s^{-1})						NO_x emission (g km^{-1} s^{-1})
	Gas car	Gas jeep	Diesel car	Diesel jeepney	Diesel bus	Gas tricycle	
2:00-3:00	1515	6	30	166	48	109	0.6
11:00-12:00	4896	48	183	1100	51	951	2.27
17:00-18:00	4109	34	222	868	40	962	1.9

Table 4. Traffic volume and NOx emission volume

6.3.3. Boundary conditions

Wind flowing into the target area and the concentrations of air pollutants in the inflowing wind were established as boundary conditions. Values measured by sensors located near the NAMRIA building were used to calculate these conditions. The average values for each period were also calculated as typical background conditions in winter from the data obtained in this experiment.

The average direction and velocity of the wind were calculated using the data collected for days between December 19 and January 9. The most frequent wind direction was chosen as the average wind direction for each period. The average wind velocity was calculated using the data when the wind direction was the same as the average wind direction. Table 5 lists the average wind direction and velocity for each period. The 1/4-power law (Peterson and Hennessey, 1978) was applied to obtain the vertical profile of the wind velocity.

Time of day	Wind Direction	Wind Velocity(ms^{-1})	Concentration(ppb)			
			NO	NO_2	O_3	NMHC
2:00-3:00	North east	0.7	15.1	9.5	4.3	407
11:00-12:00	East-northeast	4	1.2	16.9	37.2	272.3
17:00-18:00	East-northeast	2.7	15.4	19.9	11.8	407.4

Table 5. Wind direction, wind velocity and background concentration of chemical species

Average NO, NO_2, O_3, and NMHC concentrations were established as background concentrations. These chemical substances were incorporated in a photochemical reaction model that was used in this study. Their concentrations were calculated using the data for days between January 4 and 25. Data gathered at weekends were excluded from the calculation of the average background concentrations because of the difference between weekends and weekdays. Table 5 also lists the background concentrations of each pollutant for each period.

6.3.4. Photochemical reaction model

Various photochemical reaction models that consist of hundreds of elementary reactions have been previously been proposed for precisely simulating the complex chemical reaction process (Finardi et al., 2008, Kamin et al., 2008, Vuilleumier et al., 2001, Collins et al., 1997). Although these models can simulate the chemical reaction process precisely, they require long calculation times. In this study, we used the RS32 model, which consists of only 12 elementary reactions and that can be used to simulate a photochemical reaction (Tange et al., 1987). Table 6 lists the characteristics of RS32 model. Some chemical reaction velocities are proportional to light intensity; therefore, the light intensity should be estimated in order to simulate a photochemical reaction. This simulator has a function for calculating the light intensity of each grid taking the shade provided by buildings into account. The light intensity was calculated based on the altitude of the sun in Manila on January 1.

No.	Reaction	Reaction Velocity
1	$NO_2 + hv \rightarrow NO + O_3$	k1 min^{-1}
2	$NO + O_3 \rightarrow NO_2$	20.8 $ppm^{-1}min^{-1}$
3	$HC1 + O_3 \rightarrow 2RO_2 + 2HC4$	0.016 $ppm^{-1}min^{-1}$
4	$HC1 + OH \rightarrow 1.3RO_2$	25000 $ppm^{-1}min^{-1}$
5	$HC2 + OH \rightarrow 2RO_2$	3800 $ppm^{-1}min^{-1}$
6	$HC4 + OH \rightarrow RO_2$	23000 $ppm^{-1}min^{-1}$
7	$HC4 + hv \rightarrow 2RO_2$	0.01k1min^{-1}
8	$RO_2 + NO \rightarrow NO_2 + 0.4OH + 0.4RO_2 + 0.6HC4$	2500 ppm-1min-1
9	$2RO_2 \rightarrow PROD1$	5300 min^{-1}
10	$NO_2 + OH \rightarrow PROD2$	15000 $ppm^{-1}min^{-1}$
11	$O_3 + OH_2 \rightarrow PROD3$	0.046 $ppm^{-1}min^{-1}$
12	$HNO_2 + hv \rightarrow OH + NO$	0.05 k1 min^{-1}

k1:ratio of the light intensity

Table 6. RS32 photochemical reaction model

6.4. Results and discussion

Figure 17 (a), (b) and (c) show the distributions of the NO_2 concentration and wind vectors at a height of 1.5 m in the target area that were calculated based on the conditions at each period of time. The wind vectors are plotted at 40-m intervals. The NO_2 concentrations above Sen. Gil Puyat Avenue were high and gradually decreased at locations away from the avenue. The NO_2 concentration decreased at various gradients with distance from the avenue and was strongly influenced by the winds around areas near the avenue. For example, in the area south of the BOI building, where there are no buildings, the NO_2 concentration decreased appreciably with increased distance from the avenue. Meanwhile, in an area with high density of buildings, such as south of the IPO building, the NO_2 concentration decreased slightly. This indicates clearly that 3-D fluid simulators are suitable for calculating the distributions of air pollutant concentrations in an urban environment where wind flows are very complex.

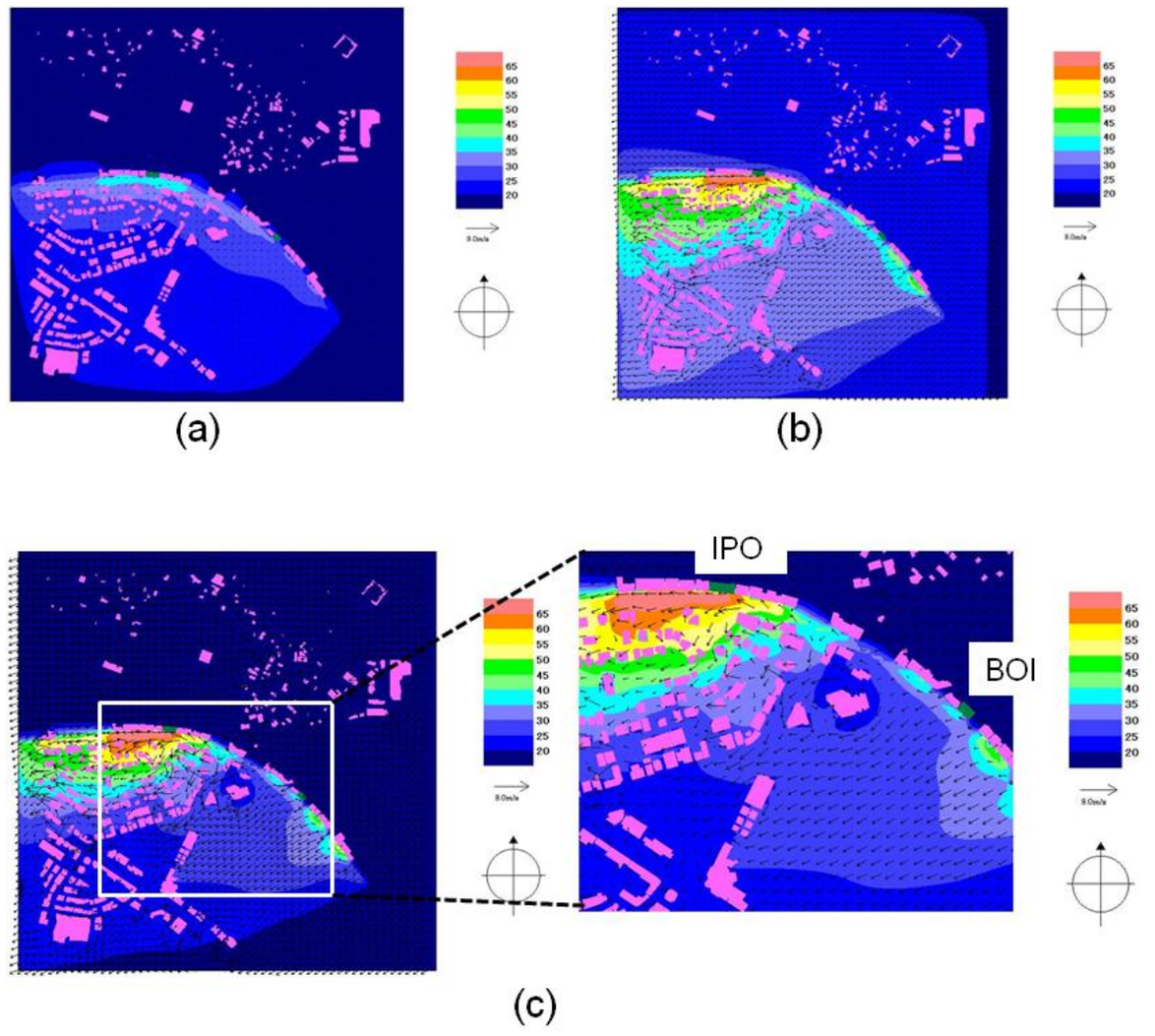

Figure 17. Distribution of NO_2 concentration (ppb) and wind vector at a height of 1.5 m in the Makati CBD. (a) Calculated results based on conditions at 2:00-3:00, (b) calculated results based on conditions at 17:00-18:00 and (c) calculated results based on conditions at 11:00-12:00

A comparison of the average NO_2 concentration of data measured on weekdays and simulated NO_2 concentrations at a height of 3.5 m in front of the IPO and BOI buildings is shown in Fig. 18 These bar charts indicate that the simulated NO_2 concentrations in front of the IPO building were close to the averages measured NO_2 concentrations. On the other hand, the simulated NO_2 concentrations in front of the BOI building based on conditions at 11:00 – 12:00 and 17:00 – 18:00 were lower than the measured averages. We infer that there are two main reasons for these differences. One is that air pollutants emitted from motor vehicles on Paseo De Roxas, which runs near the BOI building, were not considered in this study. The other reason is that the BOI building is located about 90 m from the nearest intersection. Most of us would accept that the emissions from vehicles driven in the vicinity of an intersection would exceed those of other locations on the avenues because of acceleration and idling. The simulated NO_2 concentrations were lower than the actual values because our calculation were based on the assumption that the same emission volumes were emitted regardless of the distance from the intersections. We assume that the simulation results are reliable for analyzing the effect of air pollutants emitted from vehicles on Sen. Gil Puyat Avenue. The simulated NO_2 concentrations in front of the IPO building are similar to the measured values. The simulated and measured NO_2 concentrations obtained in front of the BOI building are somewhat different as explained above.

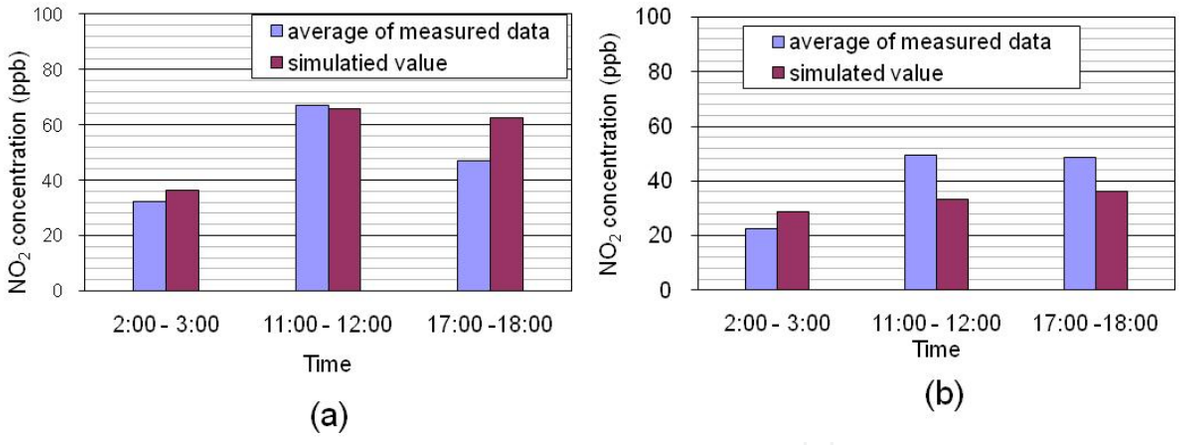

Figure 18. Comparison between average NO_2 concentration of data measured on weekdays and simulated NO_2 concentration at a height of 3.5 m in front of the building. (a) IPO, (b) BOI.

The distributions of the NO_2 concentrations around the IPO and BOI buildings that were calculated based on conditions at 11:00 – 12:00 are shown in Fig. 17(c). The NO_2 concentration in front of the IPO building was higher than that in front of the BOI building. There are high buildings on both sides of the street in front of the IPO building, thus

forming a street canyon; it is difficult for air pollutants to escape from such canyons and so they tend to have high concentrations.

We discuss the simulation results for each time period to identify areas where the NO_2 concentration exceeds the Japanese environmental quality standard levels of 40 and 60 ppb at a height of 1.5 m. The distribution of the NO_2 concentration, which was calculated based on the condition at 2:00 – 3:00, had no areas where the NO_2 concentration exceeded 40 ppb. In the distribution of the NO_2 concentration that was calculated based on the condition at 11:00 – 12:00, a high NO_2 concentration area extended to the area southwest of the IPO building. The area where the NO_2 concentration exceeded 40 ppb extended about 200 m away from the street. The area where the NO_2 concentration exceeded 60 ppb also extended about 80 m away from the street. In the distribution of the NO_2 concentrations calculated based on the condition at 17:00 – 18:00, a high NO_2 concentration area extended to the area southwest of the IPO building similar to the condition before noon. Although the amount of emission during 17:00 – 18:00 was lower than that from 11:00 – 12:00, the area where the NO_2 concentration exceeded 40 ppb was larger than the area at 11:00 – 12:00. This area extended about 300 m away from the street. On the other hand, the area where the NO_2 concentration exceeded 60 ppb was small and limited to the roadside.

An analysis of the simulation results indicates that the areas where the NO_2 concentration exceeded the standard level extended much further at noon and in the evening. We conjectured that the high-concentration areas should be larger than those in the calculated simulation results. We expect that an effort will be made to reduce air pollution by adopting such measures as improving traffic management and reinforcing the regulation of motor vehicle exhaust emissions. Meanwhile, as mentioned above, the 3-D localized fluid simulator is useful in relation to reducing the air pollutant problem because air pollutant dispersion is strongly influenced by winds around the local area.

7. Conclusion

In this project, we measured the NO_2 concentration, the SPM concentration, and the traffic volume at Makati in Manila. We also simulated the NO_2 concentration, and estimated the area with a high NO_2 concentration.

The results of our measurements and measures for reducing air pollutants are summarized below.

1. The NO_2 concentration has a tendency to increase, especially in canyon areas. One effective measure for reducing the NO_2 concentration in a canyon area is to reduce the traffic volume. For example, a 35% reduction in traffic volume can lead to a 12% reduction in NO_2 concentration.
2. The NO_2 concentration has a tendency to increase, especially in canyon areas, as already mentioned. Therefore, if it is difficult to reduce traffic volume, a city plan with open spaces instead of canyons is effective for reducing air pollutants.

3. Recently, it has been reported that certain plants have the ability to reduce air pollutants such as NO_2 (Takahashi et al., 2005). It is therefore recommended that city planners plant trees with this capability beside the road.
4. The SPM concentration depends more on traffic volume than on land use. Therefore, traffic regulation in open spaces will function successfully in reducing the mass concentration of SPM.

Author details

Yasuko Yamada Maruo and Akira Sugiyama
NTT Energy and Environment Systems Laboratories, Japan

Acknowledgement

We thank the members of this project, Mr. P. A. Varilla, Mr. R. V. Cabana and Mr. H. C. Paquiz (Commission on Information and Communications Technology), Mr. D. F. Villorente, Mr. J. C. Manio, Mr. J. Bolo, Mr. I. C. A. Lomugdang, Mr. J. S. G. Sicam, Mr. J. R. D. Ty, Mr. G. P. Guba and Mr. M. T. Patula (Advanced Science and Technology Institute), Dr. K. B. N. Vergel and Dr. J. R. F. Regidor (Affiliate National Center for Transportation Studies), Dr. J. Nakamura, Dr. S. Ogawa and Mr. S. Sakata (NTT Energy and Environment Systems Laboratories), Mr. K. Matsunaga, Mr. T. Murai and Mr. W. Ishida (Nippon Telegraph and Telephone East Corporation), Mr. S. Morimoto and Mr. M. Osaka (Nippon Telegraph and Telephone West Corporation). We appreciate the financial support provided by the APT HRD Program for Exchange of ICT Researchers/Engineers through Collaborative Research of the Ministry of Internal Affairs and Communications, Japan. We also appreciate the Live E! project in Japan for lending us the weather stations.

8. References

ADB (1992). Asian Development Bank, Vehicular emission control planning in Metro Manila Final Report.

Collins, W.J., Stevenson, D.S., Johnson, C.E. & Derwent, R.G. (1997). Tropospheric ozone in a global-scale three-dimensional Lagrangian model and its response to NOX emission controls, Journal of atmospheric chemistry, 26, 223-274.

EQS (2012) Environmental Quality Standards in Japan, 2012/02/20, Available from: http://www.env.go.jp/en/air/aq/aq.html

Finardi, S., De Maria, R., D'Allura, A., Cascone, C., Calori, G. & Lollobrigida, F. (2008). A deterministic air quality forecasting system for Torino urban area, Italy, *Environmental modeling & software*, 23, 344-355.

Isidrovaleroso, I., Monteverde, C.A. & Estoque, M.A. (1992). Diurnal-variations of air-pollution over metropolitan Manila, *Atmosfera*, 5, 142-257.

Kaminski, J. W., Neary, L., Struzewska, J., McConnell, J. C., Lupu, A., Jarosz, J., Toyota, K., Gong, S. L., Cote, J., Liu, X., Chance, K. & Richter, A. (2008). GEM-AQ, an on-line global multiscale chemical weather modelling system: model description and evaluation of gas phase chemistry processes, *Atmospheric chemistry and physics*, 8, 3255-3281.

KKE (2012) Kozo Keikaku Engineering, 2012/02/20, Available from: http://www4.kke.co.jp/kaiseki/software/air-design.html

Lodge, J.P. (1992). Air-quality in metropolitan Manila-inferences from a questionable data set, *Atmospheric Environment*, 26, 2673-2677.

Maruo, Y.Y., Ogawa, S., Ichino, T., Murao, N. & Uchiyama, M. (2003). Measurement of local variations in atmospheric nitrogen dioxide levels in Sapporo, Japan, using a new method with high spatial and high temporal resolution, *Atmospheric Environment* 37,1065-1074.

Oanh, N.T.K., Upadhyaya, N., Zhuang, Y.H., Hao, Z.P., Murthy, D.V.S., Lestari, P., Villarin, J.T., Chengchua, K., Co, H.X., Dung, N.T. & Lihdgren, E.S. (2006). Particulate air pollution in six Asian cities: Spatial and temporal distributions, and associated sources, *Atmospheric Environment*, 40, 3367-3380.

Sabin, L.D., Kozawa, K., Behrentz, E., Winer, A.M., Fitz, D.R., Pankratz, D.V., Colome, S.D., & Fruin, S.A. (2005). Analysis of real-time variable affecting children's exposure to diesel-related pollutants during school bus commutes in Los Angeles, *Atmospheric Environment*, 39, 5243-5254.

Santos, F.L., Pabroa, P.C.B., Esguerra, L.V., Racho, J.M., Almoneda, R.V. & Sucgang, R. (2006). Roadside air particulate monitoring in the PM10 range at the Poveda Learning Center, EDSA, Metro Manila, *Proceedings of the FNCA 2004 Workshop on the Utilization of Research Reactors*, 17-22.

Smith, B.J., Nitschke, M., Pilotto, L.S., Ruffin, R.E., Pisaniello, D.L. & Willson, K.J. (2000). Health effects of daily indoor nitrogen dioxide exposure in people with asthma, *European Respiratory Journal*, 16, 879-885.

Takahashi, M., Higaki, A., Nohno, M., Kamada, M., Okamura, Y., Matsui, K., Kitani, S. & Morikawa, H. (2005). Differential assimilation of nitrogen dioxide by 70 taxa of roadside trees at an urban pollution level, *Chemosphere*, 61, 633-639.

Tanaka, T., Ban., H., Ogawa, S., Maruo., Y.Y., Delaunay, J.J. & Ieyasu, T. (2004). Environment Assessment technology, *NTT Technical Review* 2, 1-5.

Tanaka., T., Gulleux, A., Ohyama, T. Maruo, Y.Y. & Hayashi, T. (1999). A ppb level NO2 gas sensor using coloration reactions in porous glass, *Sensors and Actuators* B56,247-253(1999).

Tange, H., Kataya, K., Okamoto, S. Kobayashi, K. & Yoshida, Y. (1987). Simplified photochemical reaction model for forecasting photochemical air pollution, *Industrial Pollution*, 23, 12-18(in Japanese).

Vuilleumier, L., Bamer, J.T., Harley, R.A. & Brown, N.J. (2001). Evaluation of nitrogen dioxide photolysis rates in an urban area using data from the 1997 Southern California Ozone Study, *Atmospheric Environment* 35,6525-6537.

IntechOpen